Unraveling Water's Entropic Mysteries: A Unified View of Nonpolar, Polar, and Ionic Hydration

DOR BEN-AMOTZ* AND ROBIN UNDERWOOD

*Department of Chemistry, Purdue University, West Lafayette, Indiana 47907*

RECEIVED ON JUNE 18, 2007

CONSPECTUS

Most chemical processes on earth are intimately linked to the unique properties of water, relying on the versatility with which water interacts with molecules of varying sizes and polarities. These interactions determine everything from the structure and activity of proteins and living cells to the geological partitioning of water, oil, and minerals in the Earth's crust. The role of hydrophobic hydration in the formation of biological membranes and in protein folding, as well as the importance of electrostatic interactions in the hydration of polar and ionic species, are all well known. However, the underlying molecular mechanisms of hydration are often not as well understood. This Account summarizes and extends emerging understandings of these mechanisms to reveal a newly unified view of hydration and explain previously mystifying observations. For example, rare gas atoms (e.g., Ar) and alkali-halide ions (e.g., K^+ and Cl^-) have nearly identical experimental hydration entropies, despite the significant charge-induced reorganization of water molecules.

Here, we explain how such previously mysterious observations may be understood as arising from Gibbs inequalities, which impose rigorous energetic upper and lower bounds on both hydration free energies and entropies. These fundamental Gibbs bounds depend only on the average interaction energy of a solute with water, thus providing a deep link between solute-water interaction energies and entropies. One of the surprising consequences of the emerging picture is the understanding that the hydration of an ion produces two large but nearly perfectly canceling, entropic contributions: a negative ion–water interaction entropy and a positive water reorganization entropy.

Recent work has also clarified the relationship between the strong cohesive energy of water and the free energy required to form an empty hole (cavity) in water. Here, we explain how linear response theory (whose roots may also be traced to Gibbs inequalities) can provide remarkably accurate descriptions of the process of filling aqueous cavities with nonpolar, polar, or charged molecules. The hydration of nonpolar molecules is well–described by first-order perturbation theory, which implies that turning on solute–water van der Waals interactions does not induce a significant change in water structure. The larger changes in water structure that are induced by polar and ionic solutes are well–described by second-order perturbation theory, which is equivalent to linear response theory. Comparisons of the free energies of nonpolar and polar or ionic solutes may be used to experimentally determine electrostatic contributions to water reorganization energies and entropies. The success of this approach implies that water's ability to respond to solutes of various polarities is far from saturated, as illustrated by simulations of acetonitrile (CH_3CN) in water, which reveal that even such a strongly dipolar solute only produces subtle changes in the structure of water.
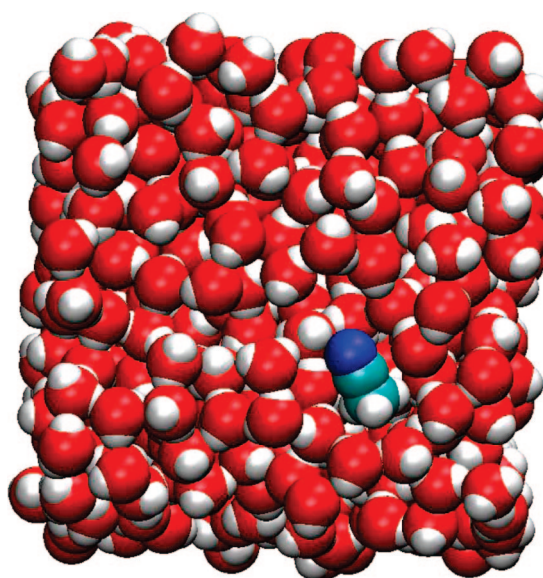
1. Introduction

Most chemical processes on earth are intimately linked to the unique properties of water and particularly the versatility with which water interacts with a wide variety of molecules. These interactions determine everything from the structure and activity of proteins and living cells to the geological partitioning of water, oil, and minerals in the earth's crust. Here we show how key features of such complex hydration processes can be understood as natural consequences of water's versatility in responding to molecules of various sizes and polarities. What emerges is a surprisingly simple and unified view of hydration, which builds on fundamental theoretical identities and inequalities, combined with experimental and simulation results.[1−8]

Unique features of hydration (as opposed to nonaqueous solvation) give rise to the remarkably varied entropic and energetic responses of water to nonpolar, polar, and charged solute molecules. These include well-known phenomena such as the marked enthalpy−entropy compensation behavior often associated with aqueous chemical equilibria[1,9−14] and the characteristically large positive partial molar heat capacities associated with hydrophobic hydration and protein denaturation,[15−18] as well as the recently highlighted dewetting (drying) of water, which occurs around idealized hydrophobic (hard-sphere) solutes larger than about 1 nm.[4,19,20] An emerging view of hydration suggests that both dispersive (van der Waals) and electrostatic (Coulombic) solute−water interactions can be well described by linear response theory,[1,2,17,21−30] which implies that water's ability to respond to solutes of widely varying polarities is far from saturated.

Here we summarize and extend these ideas, with particular emphasis on explaining the previously mystifying insensitivity of hydration entropies to solute polarity and charge.[31−33] For example, the hydration entropies of K^+ and Cl^- are virtually identical to those of Ar atoms.[31] A remarkably simple resolution of this and other related entropic mysteries emerges by recognizing an underlying anticorrelation of solute−water and water-reorganization entropies. The physical basis for this anticorrelation emerges from linear response theory,[2,22−25,27,28] whose predictions are in turn anticipated by fundamental Gibbs inequalities.[34] A broad range of experimental, simulation, and theoretical results pertaining to the hydration of nonpolar, polar, and ionic solutes are used to support and illustrate this unified view of hydration.[2,21,22,25,35−37]

2. Hydration Fundamentals

The chemical potential provides the driving force for all chemical transformations. Thus, a solute's excess chemical potential, $\mu^x = \mu_{liq} - \mu_{vap}$ dictates the influence of solvation on chemical processes, where μ_{liq} and μ_{vap} are the chemical potentials of the solute in the liquid and ideal vapor phase (at the same solute concentration). When a solute is dissolved at constant temperature and pressure, the excess chemical potential becomes equivalent to the experimental solvation Gibbs free energy $\mu^x = \Delta G$,[38] which in turn dictates the *equilibrium* solute concentration ratio in the liquid and vapor phase, $\Delta G = -RT \ln(c_{liq}/c_{vap})$. More generally, the difference between the solvation free energies of product and reactant molecules determines the effects of solvation on chemical equilibria and provides a fundamental link between chemical affinities and reaction rates.[39]

The above solvation free energy is equivalent to that of an idealized solvation process described by Ben-Naim, in which an isolated *stationary* solute is immersed in a solvent.[38] This free energy also corresponds to the reversible work associated with slowly turning on solute−solvent interactions. Although such reversible solute coupling processes are only realizable in computer simulations, they can be useful in obtaining a clearer molecular mechanistic understanding of various contributions to hydration free energies, enthalpies, and entropies.

One may envision further subdividing a hydration process into a series of reversible coupling steps in which repulsive-core (cavity), van der Waals (dispersion), and electrostatic (multipolar/ionic) interactions are sequentially introduced. At each step, the structure of water is converted from a state that we shall refer to as "unpolarized" to one that is "polarized" by the corresponding solute−water interaction, as illustrated in Figure 1. In other words, a polarized state is one whose structure has fully equilibrated in response to a given solute interaction, while an unpolarized state is one whose structure was equilibrated in the absence of the solute interaction of interest.

Solvation thermodynamic functions may contain both solute−solvent (uv) and solvent−solvent (vv) contributions. Thus, E_{uv} and E_{vv} represent the solute−solvent and solvent−solvent interaction energies, respectively, averaged over all equilibrium configurations of the fully polarized solution, while E_{uv}^0 and E_{vv}^0 are the corresponding energies averaged over all equilibrium configurations of the unpolarized solution. As we shall see, ΔG is invariably bounded above by E_{uv}^0 and below by E_{uv}.
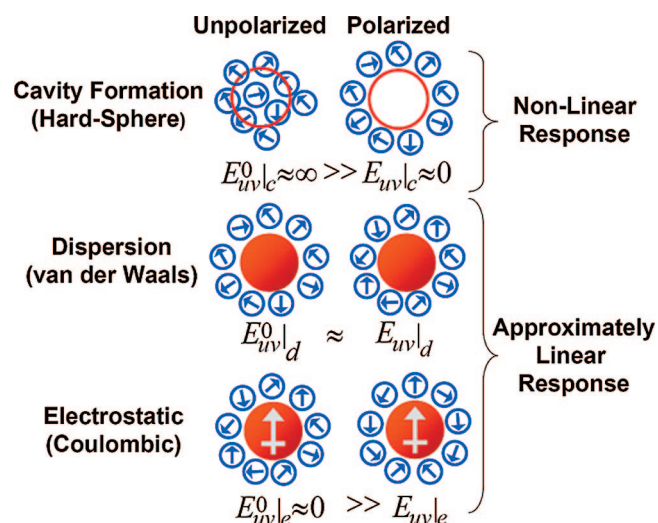
FIGURE 1. Schematic illustration of the changes in water structure and solute–water interaction energy associated with cavity formation (hard-sphere), dispersion (van der Waals), and electrostatic (Coulombic) interactions. The dipolar spheres in this picture are merely illustrative, as all of the results described in this Account pertain to actual water and solute molecules or simulations performed using realistic interaction potentials, as illustrated by the computer simulation snapshot of acetonitrile (CH_3CN) in water on the first page.

The *solvent reorganization energy* is here defined as the change in the solvent–solvent interaction energy induced by polarizing the solvent (at constant pressure), $\Delta E_{vv} = E_{vv} - E_{vv}^0$. This reorganization energy is necessarily equivalent to the corresponding solvent reorganization entropy, $T\Delta S_{vv} = T(S_{vv} - S_{vv}^0)$, as we shall see. An additional entropic contribution, S_{uv}, arises from solute–solvent energy fluctuations, as may readily be demonstrated using the Widom potential distribution theorem.[1,17] S_{uv} is necessarily negative and is proportional to the mean square deviation (fluctuation) of the solute–solvent interaction energy. In other words, a small fluctuation implies that the solute–solvent interaction energy is relatively insensitive to solvent structure, so $S_{uv} \approx 0$, while a large fluctuation implies that the solute–solvent interaction energy depends markedly on solvent structure, in which case $S_{uv} < 0$ because the associated interactions tend to decrease the range of thermally accessible solute–solvent configurations. These and other fundamental hydration thermodynamics results are summarized and further explained below, with additional details provided in the Appendix (and in recent papers).[1,2,17,18]

Experimental solvation thermodynamic functions may be expressed exactly in terms of the above intermolecular contributions.[1,2,17,18]

$$\Delta G = \mu^X = E_{uv} - TS_{uv} \tag{1}$$

$$T\Delta S = TS_{uv} + T\Delta S_{vv} \tag{2}$$

$$\Delta H = E_{uv} + \Delta E_{vv} + P\bar{v} \tag{3}$$

At ambient pressure, $P\bar{v}$ is negligibly small (where $\bar{v}$ is the solute partial molar volume), so $\Delta H \approx \Delta U = E_{uv} + \Delta E_{vv}$. More importantly, note that ΔG is expressed entirely in terms of the solute–solvent interaction energy, E_{uv}, and entropy, TS_{uv}. The experimental hydration enthalpy, ΔH, and entropy, ΔS, on the other hand, contain additional solvent reorganization contributions, ΔE_{vv} and $T\Delta S_{vv}$. This clearly implies that the solvent reorganization enthalpy and entropy must exactly cancel (compensate) when equating $\Delta G = \Delta H - T\Delta S$. In other words, *the solvent reorganization entropy and enthalpy are necessarily equivalent*, $T\Delta S_{vv} = \Delta E_{vv} + P\bar{v} \approx \Delta E_{vv}$.[1,10–13] This compensation applies to any solvation process but is particularly pertinent to hydration, which is often associated with an anomalously large reorganization energy.

Further insight into the physical significance of E_{uv}, ΔE_{vv}, TS_{uv}, and $T\Delta S_{vv}$ may be obtained by considering the first and second laws of thermodynamics, which imply that $\Delta U = \delta w + \delta q$, where δw and $\delta q = T\Delta S$ are the work and heat exchanges (between the solution and its surroundings) induced by a reversible solute coupling process (at constant T and P). Equation 2 further implies that if $\delta q/T$ is small compared to ΔS_{vv} (as we shall see is indeed often the case) then $TS_{uv} \approx -T\Delta S_{vv}$. The fundamental basis for this approximate entropic compensation will become clearer when viewed from the perspective of Gibbs inequalities (section 3) and linear response theory (section 4).

A self-solvation process, such as the hydration of a water molecule, is an important special case to which additional exact relations apply.[17,40] More specifically, for any self-solvation process

$$\Delta U = \frac{E_{uv}}{2} = -\Delta E_{vv} \tag{4}$$

so the interaction energy between a given water molecule and the surrounding water molecules, E_{uv}, is necessarily twice the experimental (constant pressure) hydration energy of water, $\Delta U \approx -41$ kJ/mol (at 298 K and 0.1 MPa).[41] This identity provides a powerful test of computer simulation predictions, yet few previous studies have utilized this fundamental self-consistency constraint (as further discussed in section 6).[42]

3. Gibbs Bounds on Hydration Free Energies and Entropies

Gibbs inequalities (also known as Bogoliubov and/or Feynman inequalities) are deeply rooted in the mathematics associated with statistically averaging exponential functions and lead to important classical and quantum mechanical variational approximation strategies.[1,3,34,43] When applied to a solvation process, these inequalities imply the following rigorous energetic bounds on solvation free energies.[2,3,43]

$$E_{uv} \leq \Delta G \leq E_{uv}^0 \quad (5)$$

Notice that this relation, combined with eq 1, further implies that $0 \leq -TS_{uv} \leq E_{uv}^0 - E_{uv}$ and thus,

$$\frac{E_{uv} - E_{uv}^0}{T} \leq S_{uv} \leq 0 \quad (6)$$

So, the solute–solvent interaction entropy, S_{uv}, *is invariably negative and has a rigorous lower bound*.

Equation 6 implies that solute–solvent coupling necessarily produces a *decrease in entropy* and a release of heat, $TS_{uv} < 0$, out into the solvent degrees of freedom. Absorption of some or all of this heat typically leads to an *increase in the entropy of the surrounding solvent* $\Delta S_{vv} = \Delta E_{vv}/T$. As a result, the net entropy change (and heat exchange) associated with a hydration process, $\Delta S = S_{uv} + \Delta S_{vv} = \delta q/T$, is often significantly smaller in magnitude than either S_{uv} or ΔS_{vv}, so $\Delta S_{vv} \approx -S_{uv}$.

The process of forming an empty spherical cavity in water is equivalent to that of inserting a hard sphere into water. Since a hard-sphere potential is, by definition, equal to zero when there is no overlap with any water molecules and infinity otherwise, it is necessarily the case that $E_{uv}|_c = 0$ and $E_{uv}^0|_c = \infty$, as illustrated schematically at the top of Figure 1. In this case, the Gibbs inequality, eq 5, is not particularly restrictive, although it does require that cavity formation free energies be invariably positive, $0 \leq \Delta G|_c \leq \infty$.

The process of turning on dispersive (van der Waals) interactions falls into an entirely different regime of the Gibbs inequalities. Note that van der Waals interactions are expected to be largely insensitive to the orientations of water molecules, as illustrated schematically in the middle of Figure 1. So, in this case eqs 5 and 6 are extremely restrictive, because they imply that $E_{uv}|_d \approx \Delta G|_d \approx E_{uv}^0|_d$ and $S_{uv}|_d \approx 0$. Thus, dispersion interactions are only expected to contribute energetically, rather than entropically, to the solvation free energies of nonpolar molecules such as rare gases and alkanes.

Electrostatic interactions, on the other hand, are quite sensitive to the orientations of water molecules, as illustrated at the bottom of Figure 1. Before water has been polarized by solute electrostatic charges, one expects solute–water electrostatic interactions to be very small, $E_{uv}^0|_e \approx 0$ (due to the cancellation of positive and negative contributions from water molecules of different orientations), while after the solvent has been polarized, the interaction energy is expected to be negative, $E_{uv}|_e < 0$ (since electrostatic interactions reorient water molecules to configurations of lower solute–solvent interaction energy).[22] Thus, in this case, eq 5 implies that $E_{uv}|_e \leq \Delta G|_e \leq 0$, while eq 6 requires that $E_{uv}|_e/T \leq S_{uv}|_e \leq 0$.

Notice that eq 5 also suggests that $\Delta G \approx (E_{uv} + E_{uv}^0)/2$ may be a reasonable approximation, particularly when E_{uv} and E_{uv}^0 do not differ greatly. This mean energy approximation also emerges from linear response theory, as further described in section 4. In other words, linear response theory may be viewed as arising from Gibbs inequalities, when ΔG is assumed to lie exactly halfway between the upper and lower bounds in eq 5.

There is also a close connection between the above mean energy approximation and thermodynamic perturbation theory. More specifically, the mean energy (linear response) approximation is equivalent to second-order perturbation theory, which in turn implies that solute–solvent energy fluctuations have an approximately Gaussian distribution.[2,22] The small energy fluctuations associated with dispersive interactions imply that such interactions are well described by first-order perturbation theory,[1,21] while the larger (but still nearly Gaussian) fluctuations associated with electrostatic interactions are well described by second-order perturbation theory.[22]

4. Linear Response Theory

The exact results in eqs 2–4 relate experimental solvation thermodynamic functions to underlying intermolecular contributions, E_{uv}, TS_{uv}, and $T\Delta S_{vv} \approx \Delta E_{vv}$. However, these relations alone are not sufficient to allow each of the latter quantities to be experimentally evaluated (except in the special case of a self-solvation process, using eq 4). Doing so requires introducing some additional information, such as that provided by linear response theory.

A linear response solvation process is one in which a constant susceptibility (slope) relates the average solute–solvent interaction energy to the associated intermolecular coupling strength.[2] In other words, linear response theory requires that the energies E_{uv}^0 and E_{uv} are linked by a linear function of the

coupling parameter that turns on the corresponding solute−solvent interactions. When combined with the well-known Kirkwood (reversible work) integral expression for $\mu^{\times}$,[1] the latter linearity implies that ΔG is the arithmetic mean of E_{uv}^{0} and E_{uv} (see Appendix for further details).[2] This linear response result, combined with eqs 1−3, immediately yields the following three remarkable identities.[2]

$$\Delta G = \frac{E_{uv} + E_{uv}^{0}}{2} \quad (7)$$

$$TS_{uv} = \frac{E_{uv} - E_{uv}^{0}}{2} \quad (8)$$

$$T\Delta S_{vv} = -TS_{uv} + \delta q \quad (9)$$

Equation 7, combined with the standard thermodynamic relation, $\Delta S = -(\partial \Delta G / \partial T)_P$, further implies that the hydration-induced heat exchange is $\delta q = T\Delta S = -T/2[(\partial E_{uv}^{0}/\partial T)_P + (\partial E_{uv}/\partial T)_P]$. Thus, the observed approximate cancellation of the solute−solvent and solvent−solvent entropies, $T\Delta S_{vv} \approx -TS_{uv}$, implies that the magnitude of δq (and the associated temperature derivatives) is relatively small, as further discussed in sections 5 and 6.

The above expressions may be applied independently to dispersive and electrostatic coupling processes (while cavity formation may be described by the aqueous cavity equation of state,[18] as further described in section 5). For dispersive interactions, we expect that $E_{uv}|_d \approx E_{uv}^{0}|_d$, while for electrostatic interactions we expect that $E_{uv}|_e \ll E_{uv}^{0}|_e \approx 0$. Thus, we may express solvation free energies and the associated reorganization energies using the following approximate identities.

$$\Delta G \approx \Delta G|_c + E_{uv}|_d + \frac{E_{uv}|_e}{2} \quad (10)$$

$$T\Delta S_{vv}|_d \approx TS_{uv}|_d \approx 0 \quad (11)$$

$$T\Delta S_{vv}|_e \approx -TS_{uv}|_e \approx \frac{-E_{uv}|_e}{2} \quad (12)$$

5. Hydration of Ionic, Polar, and Nonpolar Solutes

The most dramatic and clear confirmation of linear response predictions comes from ionic hydration experiments and simulations. Note that eq 12, combined with eq 3, suggests that electrostatic interactions are not expected to significantly contribute to experimental hydration entropies since $\Delta S|_e \approx S_{uv}|_e + \Delta S_{vv}|_e \approx 0$. This expectation is confirmed by experimental results such as those shown in the upper three panels of Fig-
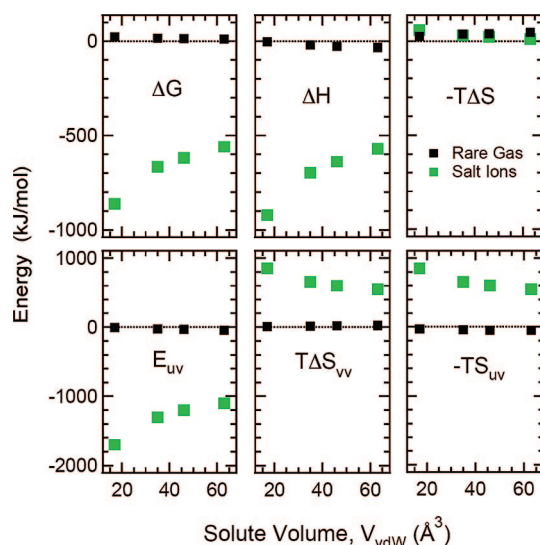

FIGURE 2. Comparison of the hydration thermodynamic functions of ions and rare gases. The green points represent results for the hydration of isolated alkali halide ions (NaF, KCl, RbBr, and CsI),[38] and the black points are the corresponding results for a pair of rare gas atoms (2Ne, 2Ar, 2Kr, and 2Xe)[38] with the same total number of electrons, plotted as a function of the van der Waals volumes of the rare gas atoms.

ure 2,[38] which compare the solvation thermodynamics of alkali-halide ions (green points) and the corresponding isoelectronic rare gas atoms (black points). These results clearly reveal the enormous electrostatic contributions to ΔG and ΔH and the strikingly small difference between the experimental hydration entropies, $T\Delta S$, of ions and rare gas atoms. Also, notice that eqs 10 and 12 suggest that the large electrostatic contribution to ΔG is approximately equivalent in magnitude to the canceling electrostatic entropy contributions, $\Delta G|_e \approx TS_{uv}|_e \approx -T\Delta S_{vv}|_e$. So, *although the measured hydration entropies of ions provide no indication of the magnitudes of the huge canceling electrostatic solute−solvent and solvent reorganization entropies, the measured free energies directly reveal just how large these are.*

More specifically, the intermolecular interaction energy and entropy contributions shown in the three lower panels in Figure 2 were extracted from the above experimental results using eqs 1−3 combined with $\Delta G|_e \approx E_{uv}/2$ (eq 10), whose approximate validity is confirmed by simulations of the hydration of a wide variety ions.[22,25,29,36,37,44] Similar, although less dramatic, confirmation of electrostatic linear response predictions also comes from the hydration of neutral polar molecules, to which we will return shortly, after first discussing the thermodynamics of cavity formation and nonpolar hydration processes.

The formation of a cavity in water is equivalent to the hydration of an idealized hard-sphere solute. Accurate expres-
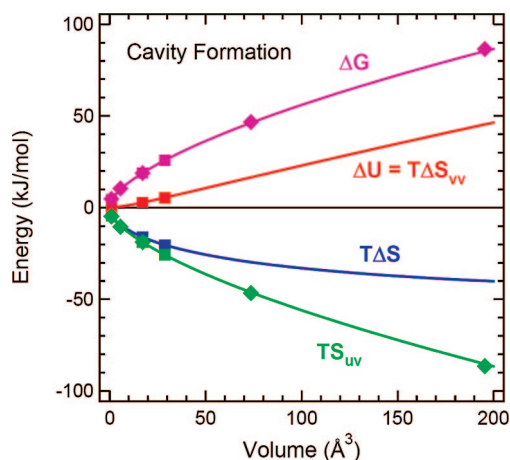
FIGURE 3. Cavity formation thermodynamics functions obtained from the C-EOS (curves) are compared with computer simulation results in SPC/E water (points).[45,46] Notice that $\Delta U = \Delta E_{vv} = \Delta H - P\bar{v} \approx \Delta H$. Only the square points were used in parametrizing the C-EOS, so the excellent agreement between curves and the larger cavity volume simulation results (diamond points) confirm the global accuracy of the C-EOS.
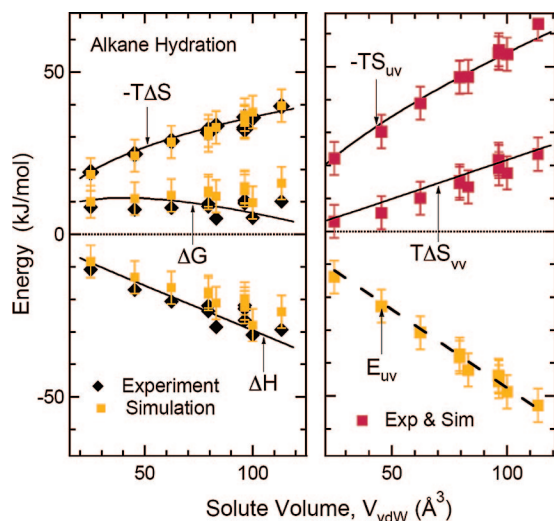

FIGURE 4. Hydration thermodynamic functions of linear (CH_4 to $n\text{-}C_6H_{14}$), branched (isobutane, isopentane, and neopentane), and cyclic (cyclopentane and cyclohexane) alkanes are plotted as a function of solute van der Waals volume. The black points represent experimental measurements,[50] the orange points are simulation results,[51,52] and the red points are obtained by combining experimental and simulation measurements. The curves represent linear response (first-order perturbation theory) predictions obtained by combining the C-EOS with simulated solute−water interactions energies (the dashed line in the right-hand panel).[18]

sions for the corresponding cavity formation thermodynamic functions, $\Delta G|_c$, $\Delta H|_c$, $\Delta S|_c$ etc., may be obtained using the recently developed aqueous cavity equation of state (C-EOS).[18] The curves in Figure 3 are C-EOS predictions, which are clearly in excellent agreement with recent computer simulation results (points).[45,46] Note that the strong hydrogen bonding of
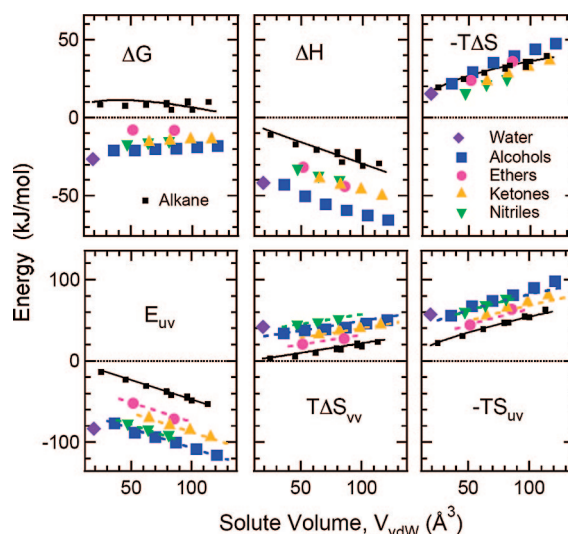

FIGURE 5. Hydration thermodynamic functions of nonpolar (black points and curves) and polar (colored points) solutes. The upper panels contain experimental results,[50] and the lower panels contain simulated E_{uv}[29] and hybrid experiment/simulation $T\Delta S_{vv}$ and $-TS_{uv}$ values, with the exception of water, for which all the results are obtained experimentally (using eq 4). Agreement with linear response predictions is evidenced by the similarity of the nonpolar and polar hydration entropies, as well as by the similar magnitudes of the differences between the polar and nonpolar values of $T\Delta S_{vv}$ and $-TS_{uv}$, both of which differ by about a factor of 2 from the corresponding differences in E_{uv}. All of these features are consistent with linear response predictions (eqs 7−12).

water leads to cavity formation thermodynamic functions that depend on cavity size in ways that differ significantly from simpler (nonpolar) fluids, as well as traditional scaled particle theory and information theory treatments of aqueous cavity formation,[47,48] particularly for large cavities. However, C-EOS predictions for cavities of molecular and macromolecular size are in quite good agreement with results obtained using a recent generalization of scaled particle theory.[45]

Experimental, simulation, and linear response predictions for the hydration of a series of linear, branched, and cyclic alkanes (at 298 K) are plotted in Figure 4 as a function of the solute van der Waals volume, V_{vdW}.[49−52] The left-hand panel shows experimental (black points) and simulated (orange points) alkane hydration thermodynamic results. The right-hand panel shows E_{uv} values obtained from simulations,[51,52] along with $T\Delta S_{vv}$ and TS_{uv} (red points) obtained by combining simulated E_{uv} values with experimental ΔG and ΔS values, using eqs 1 and 2. The dashed curve is a linear fit to the E_{uv} simulation results, which represent the average *dispersive* (Lennard-Jones) solute−solvent interaction energy. The solid curves show linear response (first-order perturbation theory) predictions obtained by combining the latter $E_{uv}|_d$ linear correlation

with the C-EOS (as further described in the Appendix).[17] *The good global agreement between the predicted curves and the experimental and simulation results for ΔG, ΔH, ΔS, TS_{uv}, and ΔE_{vv} represents a critical test and confirmation of linear response predictions.* The relatively small remaining deviations are well within the combined uncertainties of the experiments, simulations, and cavity size estimates. So, although such deviations may reflect limitations of linear response predictions, these are apparently no larger than a few kilojoules per mole (approximately $\pm RT$).

Experimental and simulation results for the hydration of various neutral polar solutes (colored points) and nonpolar solutes (black points and solid curves) are compared in Figure 5. The three upper panels show experimental hydration thermodynamic functions, while the lower three panels show simulated E_{uv} values for each solute,[29] along with TS_{uv} and $T\Delta S_{vv}$ values again obtained by combining experimental partial molar quantities with the simulated E_{uv} using eqs 1 and 2. The water self-solvation data points are exceptional, because in this case E_{uv}, TS_{uv}, and ΔE_{vv} may all be determined directly from the experimental vaporization energy[41] (using eqs 1–4). The most striking feature of the experimental results is the significant difference between ΔG and ΔH values of alkanes and polar solutes, while the corresponding $T\Delta S$ values are all quite similar. This general behavior is reminiscent of the more dramatic results shown in Figure 2. Again, the similarity of the alkane and polar hydration entropies is consistent with linear response predictions, which imply that $T\Delta S_{vv}|_e \approx -TS_{uv}|_e$, and so $T\Delta S|_e \approx TS_{uv}|_e + T\Delta S_{vv}|_e \approx 0$. Moreover, the differences between the alkane and polar hydration free energies are again found to be approximately equal to $E_{uv}|_e/2$. In other words, the difference between the colored (polar) and nonpolar (black) ΔG and ΔH results are clearly about a factor of 2 smaller than the corresponding differences between the polar and nonpolar E_{uv} curves.

The dashed curves in the lower three panels of Figure 5 represent the alkane hydration predictions shifted so as to go through the point representing the smallest polar molecule in each series. Thus, the good agreement between the points and dashed curves suggests that the effect of adding an additional methylene (CH_2) group to a hydrocarbon chain is approximately the same for both polar and nonpolar solutes, while the polarity of the headgroup produces a constant offset to the corresponding free energies and entropies. In other words, the polar head and nonpolar tail groups contribute approximately independently (additively) to hydration thermodynamics functions.

6. Conclusions and Discussion

A remarkably simple and unified view of nonpolar, polar, and ionic hydration emerges from a fundamental theoretical analysis of simulation and experimental results. This hinges on the recognition that both dispersive (van der Waals) and electrostatic (Coulombic) solute−water interactions are well described by linear response theory, as anticipated by fundamental Gibbs inequalities. This linear response behavior leads to remarkable thermodynamic relations, some of which have not previously been recognized. A particularly striking example is the nearly perfect cancellation of solute−water and water-reorganization contributions to experimental hydration entropies. More specifically, while solute−water energy fluctuations invariably produce a decrease in entropy, the resulting release of heat to the surrounding water molecules leads to an entropy increase of nearly equal and opposite magnitude. It is this entropy cancellation that is apparently responsible for the near equivalence of the experimental hydration entropies of ionic, polar, and nonpolar solutes. Moreover, the magnitude of the canceling entropies, which can be enormous, may be obtained simply by comparing the experimental hydration free energies of polar (or ionic) and nonpolar solutes of comparable size. The equal magnitudes of the two entropies also imply that the temperature derivatives of the corresponding solute−water interaction energies are small, as further discussed below.

Dispersive and electrostatic interactions fall into very different linear response regimes. Dispersive interactions are typically associated with small energy fluctuations, and thus a small entropy, while electrostatic energy fluctuations are large, and thus produce large solute−water and water-reorganization entropies (of nearly equal and opposite magnitude). The accuracy of linear response predictions implies that these fluctuations are nearly Gaussian, which in turn implies that water's capacity to respond to solutes of various polarities is far from saturated. On the other hand, the formation of a cavity of molecular size in water is not a linear process, which means that cavity formation fluctuations are significantly non-Gaussian (except for very small cavities). However, cavity formation thermodynamics may be accurately described using the C-EOS[18] or other approaches that extend beyond traditional scaled particle or information theory (Gaussian fluctuation) approximations.[4,45,48]

Although linear response predictions appear to capture the global trends and magnitudes of hydration thermodynamic functions, no molecular coupling process is expected

to be perfectly linear.[22,27,29,33,53] Moreover, the two variants of linear response theory that we have used to describe nonpolar and polar/ionic hydration are only first approximations to the full range of possible linear response behaviors. More specifically, the physically reasonable assumptions that $E_{uv}^0|_d \approx E_{uv}|_d$, $E_{uv}^0|_e \approx 0$, and $|\delta q|_e = |T/2[(\partial E_{uv}^0/\partial T)_P + (\partial E_{uv}/\partial T)_P]|_e \ll |TS_{uv}|_e \approx |T\Delta S_{vv}|_e$, are not required by linear response theory, so a broader range of linear response behaviors may in general be observed. An interesting case in point is illustrated by simulations in a wide variety of dipolar and quadrupolar fluids,[25,26] which invariably confirm the that $E_{uv}^0|_e \approx 0$, while in some polar fluids $|\delta q|_e$ (or electrostriction) is found to be non-negligible.[56] Thus, although linear response behavior is apparently a quite ubiquitous feature of electrostatic solvation (in both aqueous and nonaqueous fluids), entropy cancellation, $T\Delta S_{vv}|_e \approx -TS_{uv}|_e$ is evidently not as general, although it is clearly a characteristic feature of the electrostatic contributions to hydration under ambient conditions (which is likely linked to the large heat capacity and anomalously small thermal expansion coefficient of water). In addition to these limitations, the assumed decoupling of dispersive and electrostatic interactions, which is implicit in eq 10, is also only a convenient first approximation, as simulation results suggest that turning on electrostatic interactions can also perturb Lennard-Jones contributions to E_{uv}.[29,52] Moreover, hydration-induced changes in internal degrees of freedom and the effects of solute shape on cavity formation thermodynamics have not been explicitly considered (although these are expected to be relatively small).[1,29,54]

More accurate tests of linear response predictions require improved computer simulation measurements. For example, the constraints imposed by eq 4 may be used to critically test the absolute accuracy of simulation results for the self-solvation of water. The experimental heat of vaporization of water implies that $E_{uv} \approx -82$ kJ/mol (at 298 K and 0.1 MPa),[41] while some simulations have yielded erroneous E_{uv} values as large as -104 kJ/mol.[52] However, more recent simulations yield results that are closer to the experimental values but range from $-95 < E_{uv} < -79$ kJ/mol when different water potentials or simulation conditions are used.[42] Given all of the above possible sources of error, it is indeed remarkable that the observed deviations from linear response predictions rarely exceed about ± 10 kJ/mol (approximately $\pm 4RT$).

The experimental and simulation results presented in this Account all pertain to ambient conditions. The ubiquity of lin-

ear response solvation behavior in a wide range of dipolar and quadrupolar fluids[25,26] suggests that the electrostatic linear response approximation is likely to remain accurate in water under nonambient conditions. Experimental hydration entropies of polar and ionic solutes suggest that the magnitude of $\delta q|_e = -T/2[(\partial E_{uv}^0/\partial T)_P + (\partial E_{uv}/\partial T)_P]_e$ remains small over the biologically relevant temperature range of $0 < T < 50$ °C, while at higher temperatures the experimental hydration entropies of polar/ionic and nonpolar solutes begin to differ more significantly, implying an increase in the relative magnitude of $\delta q|_e$.

The water reorganization energy and entropy associated with cavity formation is markedly temperature dependent,[18] and this temperature dependence plays a key role in dictating the large positive hydration heat capacities of hydrophobic solutes.[17] The reorganization of water also contributes to often noted enthalpy−entropy compensation phenomena,[1,9−14] since reorganization entropies and enthalpies are rigorously compensating ($T\Delta S_{vv} = \Delta H_{vv} = \Delta E_{vv} + P\bar{v} \approx \Delta E_{vv}$). However, the results in Figures 2−5 clearly indicate that under ambient conditions the compensation of experimental hydration enthalpies and entropies only plays a marked role in hydrophobic hydration, since polar and ionic interactions lead to a large additional enthalpy but virtually no net hydration entropy (due to the entropy cancellation phenomena highlighted in this Account).

It is also interesting to note that while dispersive (van der Waals) interactions between water and relatively small solutes are well described by first-order perturbation theory, the same may not be the case for macromolecules or oil drops in water. More specifically, the significant water structural changes associated with turning on cohesive interactions between water and large hydrophobic (purely repulsive) particles[4,19,55] are expected to lead to second-order (entropic) contributions to hydration thermodynamic functions but not a breakdown of linear response behavior (as confirmed by our preliminary simulation of nanometer size oil drops in water).

In summary, the present analysis reveals fundamental links between energetic and entropic contributions to hydration, which go beyond traditional enthalpy−entropy compensation. These indicate that solute−water interaction *energies* dictate both solute−water and water−water *entropy* changes, each of which may be independently quantified by combining experimental results with linear response theory. This intimate connection between hydration energies and entropies is rooted in Gibbs inequalities, which imply that solute−solvent interaction energies

impose both upper and lower bounds on hydration entropies and free energies. These bounds ensure that cohesive intermolecular contributions to hydration can hardly stray very far from linear response predictions.

BIOGRAPHICAL INFORMATION

Dor Ben-Amotz received a B.A. from Bennington College in 1976 and a Ph.D. with Charles B. Harris from U. C. Berkeley in 1986, followed by a postdoctoral fellowship with Dudley R. Herschbach (Harvard U.) at Exxon's corporate research laboratories. He has been a professor of Physical Chemistry at Purdue University since 1989, where he has received several research and teaching awards.

Robin Underwood is a second year graduate student at Purdue University whose research is focused on liquid theory. She received a B.S. from Our Lady of the Lake University in 2005.

Appendix: Notational and Numerical Details

The following expressions relate the intermolecular interaction parameters in this work to those defined in ref 1.

$$E_{uv} = \langle \Psi \rangle^{(1)} = \varepsilon_\mu$$

$$E^0_{uv} = \langle \Psi \rangle^{(0)}$$

$$S_{uv} = -k \ln \langle e^{\beta \delta \Psi} \rangle^{(1)} = s_\mu$$

$$\Delta E_{vv} = \Delta \langle \Phi \rangle + \left[T\left(\frac{\alpha_P}{\kappa_T}\right) - P \right] \bar{v} \qquad (13)$$

Note that configuration averages in the fully coupled solution, $\langle ... \rangle^{(1)}$, are sometimes abbreviated as $\langle ... \rangle$ and $\Delta E_{vv} = \Delta \langle \Phi \rangle|_P$ is the reorganization energy at constant pressure (while $\Delta \langle \Phi \rangle = \Delta \langle \Phi \rangle|_V$ pertains to a constant-volume process).[17,18]

Linear response theory amounts to assuming that deviations (fluctuations) of the solute−solvent energy from its mean value, $\delta \Psi \equiv \Psi - \langle \Psi \rangle$, have a Gaussian distribution. When this is the case, then $\ln \langle e^{\delta \beta \Psi} \rangle = \beta^2 \langle (\delta \Psi)^2 \rangle / 2$ is independent of the value of the coupling parameter, ξ, and $\langle \Psi \rangle^{(\xi)}$ is a linear function of ξ, and thus the Kirkwood reversible work expression yields $\Delta G = \mu^x = \int_0^1 \langle \Psi \rangle^{(\xi)} d\xi = (\langle \Psi \rangle^{(0)} + \langle \Psi \rangle^{(1)})/2$.[2] Note that $\langle \Psi \rangle^{(\xi)}$ represents the *full* solute−solvent interaction energy averaged over configurations of the solvent equilibrated with a coupling parameter equal to ξ. Thus, computer simulations may be used to confirm linear response behavior by verifying either that $\langle \Psi \rangle^{(\xi)}$ is a linear function of ξ or that the interaction energy of the partially coupled solute with the solvent, $\xi \langle \Psi \rangle^{(\xi)}$, is a quadratic function of ξ.

The quantities ΔG, ΔS, ΔH, and $\bar{v}$ are equivalent to Ben-Naim's solvation thermodynamic functions ΔG^*_S, ΔS^*_S, ΔH^*_S, and $\bar{V}^*$, respectively.[38] These pertain to the solvation of a stationary solute, which may in turn be related to various other (nonstationary) solvation thermodynamic functions, as described in ref 32 and the appendix of ref 17. The experimental hydration thermodynamic functions tabulated in the Organic Compound Hydration (ORCHYD) database[50] are equivalent to those obtained using what Ben-Naim refers to as an "m-process" and so are related as follows to the above functions (at 298 K and 0.1 MPa).

$$\Delta G = \Delta_h G^0 - 7.95$$

$$\Delta H = \Delta_h H^0 + 2.29$$

$$\Delta S = \Delta_h S^0 - 34.34$$

$$\bar{v} = V_2^0 - 1.12 \qquad (14)$$

The free energy and enthalpy units are kJ/mol, while those of the entropy and volume are J/(K mol) and cm^3/mol, respectively.

In applying the C-EOS to predict cavity formation thermodynamic functions, we have used molecular van der Waals volumes, V_{vdW},[49] to estimate cavity radii, $R_c = [V_{vdW} 3/(4\pi)]^{1/3} + 1.4$ (where all lengths and volumes are expressed in angstroms units, and 1.4 is the radius of a water molecule). Simulation results for the hydration of nonpolar molecules indicate that the corresponding solute−water interaction energies are linearly correlated with solute volume, $E_{uv}|_d \approx -0.47 V_{vdW}$ at 298 K (where the energies are expressed in kJ/mol and the V_{vdW} is in Å^3 units), as indicated by the dashed line on the right-hand-side of Figure 4. The E_{uv} points in Figure 4 are previously

reported simulation results obtained using OPLS-AA solute−water potentials and a TIP4P water−water potential.[51,52] The results shown in the lower panels of Figure 5 are obtained by combining experimental ΔG and ΔH values[50] with simulation results for the corresponding solute−water electrostatic interaction energies $E_{uv}|_e$ recently reported by Almlöf, Carlsson, and Åqvist,[29] obtained using OPLS-AA and TIP3P potentials. The ionic hydration points in the lower three panels of Figure 2 are obtained as described in section 5, which is equivalent to combining the experimental results in the upper three panels with eqs 10−12. In other words, the difference between the hydration free energies of the ions and rare gases, combined with their nearly equivalent hydration entropies, are used to obtain E_{uv}, S_{uv}, and ΔS_{vv}. This procedure also implicitly assumes that cavity formation and dispersive hydration thermodynamic functions are the same for ions and the corresponding isoelectronic rare gases.

FOOTNOTES

*To whom correspondence should be addressed. E-mail: bendor@purdue.edu.

REFERENCES

1   Ben-Amotz, D.; Raineri, F.; Stell, G. Solvation thermodynamics: Theory and applications. *J. Phys. Chem. B* **2005**, *109*, 6866–6878.

2   Raineri, F. O.; Stell, G.; Ben-Amotz, D. New mean-energy formulae for free energy differences. *Mol. Phys.* **2005**, *103*, 3209–3221.

3   Isihara, A. The Gibbs-Bogoliubov inequality. *J. Phys. A (Proc. Phys. Soc.)* **1968**, *1*, 539–548.

4   Chandler, D. Interfaces and the driving force of hydrophobic assembly. *Nature* **2005**, *437*, 640–647.

5   Israelachvili, J.; Wennerstrom, H. Role of hydration and water structure in biological and colloidal interactions. *Nature* **1996**, *379*, 219–225.

6   Honig, B.; Nicholls, A. Classical electrostatics in biology and chemistry. *Science* **1995**, *268*, 1144–1149.

7   Widom, B.; Ben-Amotz, D. Note on the energy density in the solvent induced by a solute. *Proc. Natl. Acad. Sci. U.S.A.* **2006**, *103*, 18887–18890.

8   Silverstein, K. A. T.; Haymet, A. D. J.; Dill, K. A. A simple model of water and the hydrophobic effect. *J. Am. Chem. Soc.* **1998**, *120*, 3166–3175.

9   Lumry, R.; Rajender, S. Enthalpy-entropy compensation phenomena in water solutions of proteins and small molecules - a ubiquitous property of water. *Biopolymers* **1970**, *9*, 1125–1227.

10 Ben-Naim, A. A simple model for demonstrating the relation between solubility, hydrophobic interaction, and structural changes in the solvent. *J. Phys. Chem.* **1978**, *82*, 874–885.

11 Yu, H. A.; Karplus, M. A thermodynamic analysis of solvation. *J. Chem. Phys.* **1988**, *89*, 2366–2379.

12 Guillot, B.; Guissani, Y. A computer simulation study of the temperature dependence of the hydrophobic hydration. *J. Chem. Phys.* **1993**, *99*, 8075–8094.

13 Lee, B. Enthalpy-entropy compensation in the thermodynamics of hydrophobicity. *Biophys. Chem.* **1994**, *51*, 271–278.

14 Houk, K. N.; Leach, A. G.; Kim, S. P.; Zhang, X. Y. Binding affinities of host-guest, protein-ligand, and protein-transition-state complexes. *Angew. Chem., Int. Ed.* **2003**, *42*, 4872–4897.

15 Tanford, C. *The Hydrophobic Effect: Formation of Micelles and Biological Membranes*, 2nd ed.; Wiley: New York, 1980.

16 Ben-Naim, A. *Hydrophobic Interactions*; Plenum Press: New York, 1980.

17 Ben-Amotz, D.; Widom, B. Generalized solvation heat capacities. *J. Phys. Chem. B* **2006**, *110*, 19839–19849.

18 Ben-Amotz, D. Global thermodynamics of hydrophobic cavitation, dewetting, and hydration. *J. Chem. Phys.* **2005**, *123*, 184504:1−184504:8. Implementation of the C-EOS requires using β in mol/kJ units and R_c in nm units on the right-hand-side of eq A2.

19 Lum, K.; Chandler, D.; Weeks, J. D. Hydrophobicity at small and large length scales. *J. Phys. Chem. B* **1999**, *103*, 4570–4577.

20 Rajamani, S.; Truskett, T. M.; Garde, S. Hydrophobic hydration from small to large lengthscales: Understanding and manipulating the crossover. *Proc. Natl. Acad. Sci. U.S.A.* **2005**, *102*, 9475–9480.

21 Pratt, L. R.; Chandler, D. Theory of the hydrophobic effect. *J. Chem. Phys.* **1977**, *67*, 3683–3704.

22 Aqvist, J.; Hansson, T. On the validity of electrostatic linear response in polar solvents. *J. Phys. Chem.* **1996**, *100*, 9512–9521.

23 Weeks, J. D. Connecting local structure to interface formation: A molecular scale van der waals theory of nonuniform liquids. *Annu. Rev. Phys. Chem.* **2002**, *53*, 533–562.

24 Chen, Y. G.; Weeks, J. D. Local molecular field theory for effective attractions between like charged objects in systems with strong coulomb interactions. *Proc. Natl. Acad. Sci. U.S.A.* **2006**, *103*, 7560–7565.

25 Matyushov, D. V.; Ladanyi, B. M. A perturbation theory and simulations of the dipole solvation thermodynamics: Dipolar hard spheres. *J. Chem. Phys.* **1999**, *110*, 994–1009.

26 Matyushov, D. V.; Voth, G. A. A perturbation theory for solvation thermodynamics: Dipolar-quadrupolar liquids. *J. Chem. Phys.* **1999**, *111*, 3630–3638.

27 Ghorai, P. K.; Matyushov, D. V. Solvent reorganization entropy of electron transfer in polar solvents. *J. Phys. Chem. A* **2006**, *110*, 8857–8863.

28 Paliwal, A.; Asthagiri, D.; Pratt, L. R.; Ashbaugh, H. S.; Paulaitis, M. E. An analysis of molecular packing and chemical association in liquid water using quasichemical theory. *J. Chem. Phys.* **2006**, *124*, 224502:1−224502:7.

29 Almlof, M.; Carlsson, J.; Aqvist, J. Improving the accuracy of the linear interaction energy method for solvation free energies. *J. Chem. Theory Comput.* **2007**, *3*, 2162–2175.

30 Deng, Y. Q.; Roux, B. Hydration of amino acid side chains: Nonpolar and electrostatic contributions calculated from staged molecular dynamics free energy simulations with explicit water molecules. *J. Phys. Chem. B* **2004**, *108*, 16567–16576.

31 Friedman, H. L.; Krishnan, C. V. In *Aqueous Solutions of Simple Electrolytes*; Franks, F., Ed.; Water, a Comprehensive Treatise, Vol. 3; Plenum: London, 1973; pp 1−118.

32 Ashbaugh, H. S.; Asthagiri, D.; Pratt, L. R.; Rempe, S. B. Hydration of krypton and consideration of clathrate models of hydrophobic effects from the perspective of quasi-chemical theory. *Biophys. Chem.* **2003**, *105*, 323–338.

33 Lynden-Bell, R. M.; Rasaiah, J. C.; Noworyta, J. P. Using simulation to study solvation in water. *Pure Appl. Chem.* **2001**, *73*, 1721–1731.

34 Weeks, J. D. External fields, density functionals, and the gibbs inequality. *J. Stat. Phys.* **2003**, *110*, 1209–1218.

35 Pratt, L. R.; Chandler, D. Theoretical and computational studies of hydrophobic interactions. *Methods Enzymol.* **1986**, *127*, 48–63.

36 King, G.; Barford, R. A. Calculation of electrostatic free-energy differences with a time-saving approximate method. *J. Phys. Chem.* **1993**, *97*, 8798–8802.

37 Carlson, H. A.; Jorgensen, W. L. An extended linear-response method for determining free-energies of hydration. *J. Phys. Chem.* **1995**, *99*, 10667–10673.

38 Ben-Naim, A. *Solvation Thermodynamics*; Plenum Press: New York, 1987.

39 Kondepudi, D.; Prigogine, I. *Modern Thermodynamics. From heat Engines to Dissipative Structures*; John Wiley and Sons: New York, 1998.

40 Stone, M. T.; Veld, P. J.; Lu, Y.; Sanchez, I. C. Hydrophobic/hydrophilic solvation: Inferences from Monte Carlo simulations and experiments. *Mol. Phys.* **2002**, *100*, 2773–2792.

41 Lemmon, E. W.; Huber, M. L.; McLinden, M. O. NIST Standard Reference Database 23, Version 8.0, National Institute of Standards and Technology: Boulder, CO, 2007.

42 van der Spoel, D.; van Maaren, P. J. The origin of layer structure artifacts in simulations of liquid water. *J. Chem. Theory Comput.* **2006**, *2*, 1–11.

43 Hansen, J. P.; McDonald, I. R. *Theory of Simple Liquids*, 3rd ed.; Academic Press: New York, 2006.

44 Westergren, J.; Lindfors, L.; Hoglund, T.; Luder, K.; Nordholm, S.; Kjellander, R. In silico prediction of drug solubility: 1. Free energy of hydration. *J. Phys. Chem. B* **2007**, *111*, 1872–1882.

45 Ashbaugh, H. S.; Pratt, L. R. Colloquium: Scaled particle theory and the length scales of hydrophobicity. *Rev. Mod. Phys.* **2006**, *78*, 159–178.

46 Huang, D. M.; Geissler, P. L.; Chandler, D. Scaling of hydrophobic solvation free energies. *J. Phys. Chem. B* **2001**, *105*, 6704–6709.

47 Pierotti, R. A. Scaled particle theory of aqueous and non-aqueous solutions. *Chem. Rev.* **1976**, *76*, 717–726.

48 Hummer, G.; Garde, S.; Garcia, A. E.; Paulaitis, M. E.; Pratt, L. R. Hydrophobic effects on a molecular scale. *J. Phys. Chem. B* **1998**, *102*, 10469–10482.

49 Bondi, A. Van der waals volumes and radii. *J. Phys. Chem.* **1964**, *68*, 441–451.

50 Plyasunov, N. V.; Plyasunov, A. V.; Shock, E. L. Database of thermodynamic properties for aqueous organic compounds. *Int. J. Thermophys.* **2004**, *25*, 351–360; http://webdocs.asu.edu.

51 Gallicchio, E.; Kubo, M. M.; Levy, R. M. Enthalpy-entropy and cavity decomposition of alkane hydration free energies: Numerical results and implications for theories of hydrophobic solvation. *J. Phys. Chem. B* **2000**, *104*, 6271–6285.

52 Duffy, E. M.; Jorgensen, W. L. Prediction of properties from simulations: Free energies of solvation in hexadecane, octanol, and water. *J. Am. Chem. Soc.* **2000**, *122*, 2878–2888.

53 Nina, M.; Beglov, D.; Roux, B. Atomic radii for continuum electrostatics calculations based on molecular dynamics free energy simulations. *J. Phys. Chem. B* **1997**, *101*, 5239–5248.

54 Ben-Amotz, D.; Omelyan, I. P. The influence of molecular shape on chemical reaction thermodynamics. *J. Chem. Phys.* **2001**, *115*, 9401–9409.

55 Huang, D. M.; Chandler, D. The hydrophobic effect and the influence of solute-solvent attractions. *J. Phys. Chem. B* **2002**, *106*, 2047–2053.

56 The dipolar and quadrupolar solvation simulations of Matyushov and co-workers (refs 25−27) indicate that $0.9 < \chi_{NL} = 2TS_{uv}/E_{uv} < 1.1$, while $0.5 < \chi_s = -2\Delta E_{vv}/E_{uv} < 0.9$. Linear response theory combined with $E_{uv}^0|_e \approx 0$ implies that $\chi_{NL} = 1$ while $\chi_s = 1$ is predicted when $|\delta q|_e \approx 0$ and electrostatic interactions do not significantly change the partial molar volume of the solute (i.e., electrostriction is negligible). Thus, electrostatic entropy cancelation is apparently less general than $E_{uv}^0|_e \approx 0$.